PERGAMON

International Journal of Heat and Mass Transfer 42 (1999) 3431–3445

International Journal of HEAT and MASS TRANSFER

Influence of molecular vibration and transport model on computation of the wall heat flux

Gennaro Zuppardi[a,*], Federico De Filippis[b]

[a]*Dipartimento di Scienza ed Ingegneria dello Spazio, "Luigi G. Napolitano", P. le V. Tecchio 80, 80125 Naples, Italy*
[b]*Plasma Wind Tunnel Section, Centro Italiano Ricerche Aerospaziali, Via Maiorise, 81043 Capua, Italy*

Received 26 June 1998; received in revised form 21 December 1998

Abstract

Zuppardi and Verde (Improved Fay–Riddell prcoedure to compute the stagnation point heat flux, Journal of Spacecraft and Rockets 35(3) (1998) 403–405) introduced some operating improvements in the Fay–Riddell computing procedure for the solution of the laminar boundary layer and for the computation of the heat flux at the stagnation point of spherical bodies in high speed, non-equilibrium dissociating air. Zuppardi and Verde pointed out that the most important improvements were related to the computation both of vibrational temperatures and of Prandtl and Lewis numbers. Vibrational temperatures were computed only as functions of the free stream thermodynamic parameters. Prandtl and Lewis numbers were computed as functions of both the free stream and the local thermodynamic parameters in the boundary layer. The Chapman–Enskog theory with the Lennard–Jones collision integrals were used to compute the transport coefficients. In the present paper the effects of the variability of the vibrational temperatures also in the boundary layer, and of using the more updated collision integrals by Yun and Mason (Collision integrals for the transport properties of dissociating air at high temperature, The Physics of Fluid 5(4) (1962) 380–386) have been evaluated. The results showed that the influence of these factors on the profile of the thermo-fluid–dynamic parameters in the boundary layer was negligible, but it was important on the wall heat flux. The inclusion of the variability of molecular vibration improved the matching both with Navier–Stokes results and experimental data.

1. Introduction

The evaluation of the heat flux, entering a space vehicle during the re-entry path, is one of the most important problems in the design of the vehicle and, more specifically, of the Thermal Protection System (TPS). The velocity of a capsule, at an altitude of 60 km (ambient density $= 1.03 \times 10^{-3}$ kg/m^3, ambient temperature $= 275$ K [1]), is about 7000 m/s (Mach number $\cong 21$, Reynolds number per meter $\cong 4 \times 10^5$, total flow enthalpy $\cong 25$ MJ/kg); the heat flux, entering the capsule, is on the order of 1000 kW/m^2.

Since the beginning of the 'space age' several methodologies have been developed to compute the wall heat flux in non-equilibrium gases, where dissociation and ionization processes can occur. Fay and Riddell [2] is a pioneering work in the field of the aero-thermo-chemistry of dissociating gases and of the evaluation of the heat flux at the stagnation point of spherical bodies. By correlating a massive number of calculations, covering a wide range of: wall temperatures, altitudes (i.e. ambient temperatures and ambient densities), flight velocities, wall conditions (catalytic, non-catalytic), states of the gas (equilibrium, non-equi-

* Corresponding author.

0017-9310/99/$ - see front matter
PII: S0017-9310(99)00030-7

Nomenclature

C	mass fraction
c	molar fraction
c_p	specific heat at constant pressure, J/kg/K
d	characteristic collision diameter, Å
D	diffusion coefficient m^2/s
e	internal energy per unit mass, J/kg
f	non-dimensional stream function
h	enthalpy per unit mass, J/kg
h_P	Planck constant (6.63×10^{-34} J s)
h_0	total enthalpy per unit mass, J/kg
k	thermal conductivity, W/m/K
k_B	Boltzmann constant (1.38×10^{-23} J/K)
K	recombination rate constant, m^6/kg $mole^2$/s
Le	Lewis number ($Le = \rho D c_p/k$)
m	molecular weight, kg/kg mole
p	pressure, Pa
$\dot{q}$	heat flux, W/m^2
$\dot{q}_N$	normalized heat flux, $J/cm^{3/2}/s/atm^{1/2}$
r	cylindrical body radius, m
R	gas constant, J/kg/K
R_b	body nose radius, m
R_0	universal gas constant (8314 J/kg mole/K)
s	ratio of current mass fraction and mass fraction at the boundary layer edge
t	time, s
T	temperature, K
u	x component of velocity, m/s
x, y	distance along and normal to the body surface, m.

Greek symbols

α_1	constant defining the characteristic vibrational time, atm s [see Eq. (18)]
α_2	constant defining the characteristic vibrational time, K [see Eq. (18)]
δ	boundary layer thickness, m
Δh°	heat of formation at 0 K, J/kg
ϵ	characteristic energy of interaction between the molecules, J
η_δ	boundary layer thickness in transformed co-ordinate
ϑ	non-dimensional temperature ($\vartheta = T/T_e$)
μ	viscosity, kg/m/s
ν	molecule vibrational frequency, 1/s
ξ, η	transformed space variables [see Eqs. (1a) and (b)]
ρ	density, kg/m^3
τ	non-dimensional vibrational relaxation time
Ω_D	collision integral for diffusivity
Ω_μ	collision integral for viscosity.

Subscripts and superscripts

A	atom
c	characteristic
e	boundary layer edge
E	equilibrium
i, j	ith, jth mixture species
M	molecule
s	stagnation point in external flow

T	thermal
v	vibrational
w	wall
∞	free stream
$'$	derivation with respect to η
$\bar{}$	average with respect to the gas composition.

librium), Fay and Riddell [2] obtained formulas allowing the computation of the wall heat flux. These formulas are used still today to get preliminary information on aerodynamic heating.

Zuppardi and Verde [3] improved the Fay–Riddell computing procedure. In fact, even though the original Fay–Riddell procedure relies on theoretically sound bases, it suffers from inaccuracies that can reduce the validity of the results and therefore, of the above mentioned correlation formulas. These shortcomings were due to the lack of computer resources at that time (1958), the scarce knowledge about kinetic parameters, like the recombination/dissociation rates and vibrational temperatures, transport coefficients, thermodynamic parameters, and so on. More specifically Zuppardi and Verde [3] pointed out that the values both of vibrational temperatures and of Prandtl and Lewis numbers were the most important improvements in the solution of the boundary layer equations and therefore, in the computation of the wall heat flux. Fay and Riddell [2] proposed to use constant and non realistic values of both vibrational temperature (800 K), Prandtl number (0.71) and Lewis number (1, 1.4, 2). In the Zuppardi–Verde procedure: (i) vibrational temperatures are considered to be variable with the free stream thermodynamic parameters, (ii) Prandtl and Lewis numbers are computed as a function of both the free stream and the local thermodynamic parameters in the boundary layers. The transport coefficients were computed by the Chapman–Enskog theory, with the Lennard–Jones collision integrals [4,5].

In the present paper the influence, on computation of the boundary layer parameters and of the wall heat flux, of the variability of the vibrational temperatures also in the boundary layer and of using the more updated collision integrals by Yun and Mason [6] in the Chapman–Enskog theory is evaluated. The aim of the present paper, that has to be considered as the logic continuation of the work by Zuppardi and Verde [3], is to improve the reliability of the Zuppardi–Verde procedure and therefore, to provide the hypersonic wind tunnel experimenter with an easy tool, computing reliable results with which to compare the experimental data and, moreover, to get an insight into the catalycity of the surface of the test model [7]. The computer code, developed on the present procedure in fact, can also run on personal computers.

The code was run with flow total enthalpy up to about 40 MJ/kg. The gas is a mixture of nitrogen and oxygen with a composition very close to air. The stagnation point heat fluxes, computed considering the gas in non-equilibrium and a fully catalytic wall, compare successfully both with numerical results by a Navier–Stokes code and with experimental data.

2. Fay–Riddell procedure

The Fay–Riddell procedure solves the equations of a laminar, steady boundary layer at the stagnation point of a spherical body in a very high speed flow and in non-equilibrium dissociating gas. The balance equations of momentum, energy and species continuity are solved by the self-similar solutions theory.

The independent space variables x and y are transformed by the Lees–Dorodnitsyn transformation in ξ and η variables. These read:

$$\eta = \frac{r u_e}{\sqrt{2\xi}} \int_0^y \rho \, dy \tag{1a}$$

$$\xi = \int_0^x \rho_w \mu_w u_e r^2 \, dx \tag{1b}$$

Fig. 1 sketches the physical model. The Fay–Riddell procedure considers air just as a one-component gas; the gas is a binary mixture of 'air' atoms and 'air' molecules. This assumption simplifies the problem because it reduces the number of equations of species continuity to one. The non-dimensional, dependent variables are f, ϑ and C_A, where f is defined in such a way that $f' = u/u_e$. The system of ordinary differential equations is reported here for convenience:

$$\text{Momentum:} \quad (\lambda f'')' + f f'' + 0.5[\zeta - f'^2] = 0 \tag{2}$$

$$\text{Energy:} \quad ((\sigma\lambda/Pr)\vartheta')' + \sigma f \vartheta' + \beta(Le\,\lambda/Pr)\vartheta' C'_A + \chi_1\chi_2\nu = 0 \tag{3}$$

$$\text{Atom continuity:} \quad ((\lambda\, Le/Pr)C'_A)' + f C'_A - \chi_1\nu = 0 \tag{4}$$

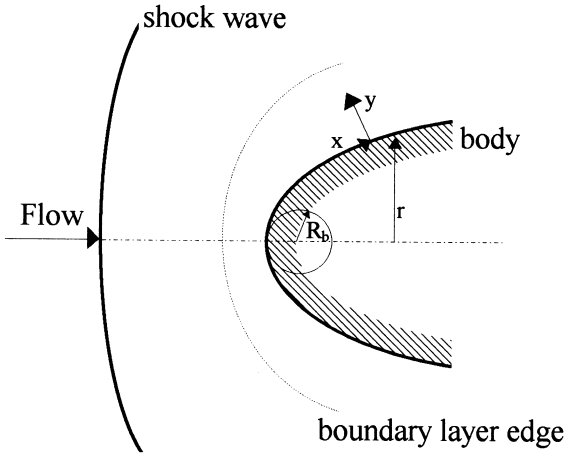

Fig. 1. Sketch of the physical model.

where: ζ, λ, β, σ, ν, χ_1 and χ_2 are defined, and then computed by Fay and Riddell [2] (on the above mentioned assumption that the gas is a binary mixture of 'air' atoms and 'air' molecules) as:

$$\zeta = \rho_s/\rho = [(1 + C_A)/(1 + C_{As})]\vartheta \tag{5}$$

$$\lambda = \rho\mu/\rho_w\mu_w = [1/(1 + C_A)]^{1/5}(\vartheta_w/\vartheta)F(\vartheta) \tag{6}$$

where

$$F(\vartheta) = (T_s\vartheta/300)^{1.5}[413/(T_s\vartheta + 113)] + 3.7(T_s\vartheta/10^4)^2 - 2.35(T_s\vartheta/10^4)^4 \tag{7}$$

is a fitted curve giving the temperature dependence of the viscosity under the assumption that atoms and molecules have the same collision cross-section,

$$\beta = (c_{pA} - c_{pM})/\bar{c}_{pw} = 3/7 - 2/7\, e^{-(\vartheta_v/\vartheta)^2} \tag{8}$$

$$\sigma = \bar{c}_p/\bar{c}_{pw} = 10/7C_A + [1 + 2/7\, e^{-(\vartheta_v/\vartheta)^2}](1 - C_A) \tag{9}$$

$$\nu = (C_A^2 - C_{AE}^2)/\vartheta^{3.5}(1 + C_A) \tag{10}$$

$$\chi_1 = Kp_s^2 T_s^{-3.5} R_0^{-2}(du_e/dx)_s^{-1} \tag{11}$$

where the velocity gradient at the stagnation point is computed by the Newtonian theory as:

$$(du_e/dx)_s = 1/R_b\sqrt{2(p_s - p_\infty)/\rho_s} \tag{12}$$

$$\chi_2 = h_D/(\bar{c}_{pw}T_s) \tag{13}$$

where h_D is the average atomic dissociation enthalpy in external flow:

$$h_D = \sum_i C_{is}\Delta h_i^0 \tag{14}$$

The boundary conditions are:

- at the wall: $(f)_w = 0$, $(df/d\eta)_w = 0$, $(\vartheta)_w = \vartheta_w$
- at the wall for a fully catalytic wall: $(C_A)_w = 0$
- at the boundary layer edge: $(df/d\eta)_e = 1$, $(\vartheta)_e = 1$, $(C_A)_e = C_{As}$

The computing approximations made by Fay–Riddell have been used also in the Zuppardi–Verde procedure. Eqs. (5)–(10) are very useful from an operative point of view. More specifically Eqs. (6) and (9) are useful in developing the derivatives in the boundary layer equations. As shown later, these approximations do not influence the goodness of results.

In the Zuppardi–Verde procedure the gas is a mixture of five chemical species: O_2, N_2, NO, O and N. Since the Fay–Riddell equations work on the global atom mass fraction (C_A), the current mass fractions of O and N are evaluated, approximately, by scaling the value of C_A by the free stream mass fraction of oxygen and nitrogen. The current mass fractions of O_2, N_2 and NO are then evaluated by the continuity equation of each species. Moreover, even though Eqs. (2)–(4) were obtained by Fay and Riddell [2] by assuming the Prandtl and Lewis numbers constant, the equations are integrated by considering these numbers variable in the boundary layer.

In a dissociating, viscous gas flow the wall heat flux is due to the sum of a conductive term [first term in Eq. (15)], and a diffusive transport of energy associated to atoms recombining at the wall; the recombination process is exothermic. The diffusive transport is due to Fick's law (second term) and to a thermal diffusion (third term).

$$\dot{q}_w = (k\,\partial T/\partial y)_w + \left(\sum_i \rho D_i(h_i - \Delta h_i^0)\,\partial C_{Ai}/\partial y\right)_w + \left(\sum_i \rho D_i^T C_{Ai}/T(h_i - \Delta h_i^0)\,\partial T/\partial y\right)_w \tag{15}$$

Fay and Riddell [2] specialized Eq. (15) to compute the heat flux at the stagnation point of spherical bodies. By working out Eq. (15) in terms of non-dimensional temperature, Lewis numbers, Prandtl number, ratios of current mass fraction and mass fraction at the boundary layer edge, wall enthalpy and enthalpy at the boundary layer edge, they provided the following equation, matching the boundary layer computing procedure:

$$\dot{q}_w = [\sqrt{2}\bar{c}_{pw}T_s/(h_s - h_w)] \times \left\{ \vartheta' + \sum_i C^i_{As}(h_i - \Delta h^0_i)/\bar{c}_p T_s \times (Le_i\, s'_i + Le^T_i\, s_i \vartheta'/\vartheta) \right\}_{\eta=0}$$

$$\sqrt{\rho_w \mu_w (du_e/dx)_s}[(h_s - h_w)/Pr] \quad (16)$$

Thermal diffusion was neglected (i.e. $Le^T_i = 0$) in all numerical computations, reported in this paper.

3. Molecular vibration

The equation, for the vibrational energy of the three di-atomic species, is:

$$\frac{de_{vi}}{dt} = \frac{1}{t_{vi}}(e^E_{vi} - e_{vi}) \quad i = O_2, N_2, NO \quad (17)$$

Anderson [4] suggests to compute the vibrational relaxation time (t_{vi}) by:

$$t_{vi} = \frac{\alpha_{1i}\, e^{(\alpha_{2i}/T)^{1/3}}}{p} \quad (18)$$

where α_{1i} [atm s] and α_{2i} [K] are constants, pressure p is in atm. The specific vibrational energy e_{vi} is:

$$e_{vi} = \frac{h_P \nu_i/k_B T}{e^{h_P \nu_i/k_B T} - 1} RT \quad (19)$$

To be included in the present computing procedure, Eq. (17) has to be written in terms of non-dimensional temperatures (ϑ, ϑ_{vi}) and non-dimensional space variable (η).

Times t_{vi} are made non-dimensional by a reference time t_r ($\tau_i = t_{vi}/t_r$). This is computed as the ratio of the boundary layer thickness and the tangential velocity at the boundary layer edge:

$$t_r = \frac{\delta}{u_e} \quad (20)$$

For a very small x, u_e can be computed by:

$$u_e = \left(\frac{du_e}{dx}\right)_s x \quad (21)$$

The boundary layer thickness is computed by Eqs. (1a) and (b). Since $r \cong x$ (Fig. 1) then:

$$\xi = \rho_w \mu_w \left(\frac{du_e}{dx}\right)_s \frac{x^4}{4} \quad (22)$$

By using in the integral of Eq. (1b) for the density the average, constant value $\bar{\rho} = (\rho_e + \rho_w)/2$:

$$\delta = \eta_\delta \frac{\sqrt{2\xi}}{x u_e} \frac{1}{\bar{\rho}} \quad (23)$$

Eq. (17) in terms of non-dimensional time derivatives and of non-dimensional temperatures is transformed in a non-dimensional space derivative by dividing by a non-dimensional velocity:

$$\frac{d\vartheta_{vi}}{d\eta} = \frac{1}{\tau_i}\left[\frac{\vartheta^c_{vi}}{e^{(\vartheta^c_{vi}/\vartheta)} - 1} - \frac{\vartheta^c_{vi}}{e^{(\vartheta^c_{vi}/\vartheta_{vi})} - 1}\right] \Big/ \frac{df}{d\eta} \quad (24)$$

The weighted average of both non-dimensional space derivatives and non-dimensional vibration temperatures are used in Eqs. (2)–(4). The vibration and dissociation/recombination processes of di-atomic species are considered uncoupled.

4. Transport models

The transport coefficients are computed as functions of temperature and pressure, by the Chapman–Enskog theory. According to this theory, the viscosity and the thermal conductivity of a pure gas are:

$$\mu_i = \frac{2.6693 \times 10^{-6}\sqrt{m_i T}}{d_i^2 \Omega_{\mu_i}} \quad i = O_2, N_2, NO, O, N \quad (25)$$

$$k_i = \left(c_{pi} + \frac{5}{4}\frac{R_0}{m_i}\right)\mu_i \quad (26)$$

The binary diffusion coefficient of the i–j pair is:

$$D_{i,j} = 1.8583 \times 10^{-7} \frac{\sqrt{T^3\left(\frac{1}{m_i} + \frac{1}{m_j}\right)}}{p d^2_{i,j} \Omega_{D_{i,j}}} \quad j = O_2, N_2, NO, O, N \quad (27)$$

where pressure p is in atm.

The former Zuppardi–Verde procedure uses in Eqs. (25) and (27) the Lennard–Jones collision integrals. Both Ω_{μ_i} and $\Omega_{D_{i,j}}$ are evaluated as a function of the non-dimensional parameter $k_B T/\epsilon_i$ and $k_B T/\epsilon_{i,j}$, respectively, where $\epsilon_{i,j} = \sqrt{\epsilon_i \epsilon_j}$ and $d_{i,j} = 0.5(d_i + d_j)$. Values of ϵ_i, d_i, Ω_{μ_i} and $\Omega_{D_{i,j}}$ are tabulated in [4] and [5].

An alternative way to calculate the transport coefficients by the Chapman–Enskog theory, is to use the collision integrals by Yun and Mason [6]. In this case $d_i^2\Omega_{\mu_i}$ and $d^2_{i,j}\Omega_{D_{i,j}}$ are tabulated for each species and each pair or species, respectively, as a function of temperature. These integrals look to be more accurate than the Lennard–Jones ones. In fact the Lennard–

Jones collision integrals rely, for every species, on the same dependence law from temperature. On the contrary the Yun–Mason collision integrals rely on more updated dependence law from temperature, specific for each species.

The viscosity and the thermal conductivity of the mixture are evaluated, from the coefficients of each species and the local gas composition, by the Wilke rule [4,5]:

$$\mu = \sum_{i=1}^{n} \frac{c_i \mu_i}{\sum_{j=1}^{n} c_j \Phi_{i,j}} \tag{28}$$

where

$$\Phi_{i,j} = \frac{1}{\sqrt{8}} \left(1 + \frac{m_i}{m_j}\right)^{-1/2} \left[1 + \left(\frac{\mu_i}{\mu_j}\right)^{1/2} \left(\frac{m_j}{m_i}\right)^{1/4}\right]^2 \tag{29}$$

When the Lennard–Jones collision integrals are used, the mixture mass diffusivity is computed by using, for the parameters defining the diffusion coefficient, the average values weighted with respect to the gas composition (self-diffusivity coefficient [5]). When the Yun–Mason collision integrals are used, the binary diffusivity of molecular nitrogen in atomic nitrogen is considered as representative of the mixture self-diffusivity.

The transport coefficients of the mixture are used to compute the Prandtl number and the Lewis number. The partial Lewis numbers (Le_i) are computed by using the mixture constant pressure specific heat ($\bar{c}_p$), the mixture thermal conductivity ($\bar{k}$) and the mass diffusivity of each species in the mixture (D_i). These are [4,5]:

$$D_i = \frac{1 - c_i}{\sum_{j=1}^{n} \frac{c_j}{D_{i,j}}} \tag{30}$$

The thermal diffusivities, and therefore, the related Lewis numbers, have been neglected in the computation of the wall heat flux.

5. Description of the pre-processor

In order to work in physically congruent conditions, in terms of temperature, density, gas composition and so on, the present code, has been interfaced with a computer code [8], modelling the jet of an arc wind tunnel. The tunnel is supposed to be made of a heater, a chamber to mix hot nitrogen (coming from the heater) and cold oxygen, and a supersonic nozzle (area ratio 1:4). It solves a one-dimensional, steady, inviscid flow field. The gas is a mixture of five species (O_2, N_2, NO, O, N) in chemical and vibrational non-equilibrium. The thermo-chemical model considers the recombination/dissociation and the vibration of diatomic molecules and relies on the same rate parameters [9], used in the present code.

The thermo-fluid–dynamic parameters and the gas composition at the nozzle exit are considered as the free stream values. The parameters, at the stagnation point boundary layer edge, are those downstream of a normal shock wave, due to a sphere model. The gas composition and the vibrational temperatures are supposed to be frozen both through the shock and along the stand-off distance up to the boundary layer edge (no relevant chemical relaxation process was found). The total enthalpy at the stagnation point is that of the free stream ($h_{0s} = h_{0\infty}$).

The code run with a free stream total enthalpy ($h_{0\infty}$) up to about 40 MJ/kg. More specifically the data shown here are related to the following five values of $h_{0\infty}$: 3, 12, 22, 31, 37 MJ/kg. The input gas is simulated air; the mass fractions of oxygen and nitrogen are 0.20 and 0.80, respectively. Some free stream thermo-fluid–dynamic parameters are reported in Table 1. The free stream Mach number changes from 3.0–3.3 in the range of total enthalpy.

6. Comparison data

The present results are compared both with numerical results and experimental data, in terms of normalized heat flux $\dot{q}_N$ as a function of the enthalpy potential ($h_{0\infty} - h_w$) [10]:

Table 1
Free stream thermo-fluid–dynamic parameters

$h_{0\infty}$ [MJ/kg]	V_∞ [m/s]	T_∞ [K]	ρ_∞ [kg/m^3]	$\bar{T}_{v\infty}$ [K]	C_{O_2}	C_O	C_{N_2}	C_N	C_{NO}
3	1927	1053	2.2×10^{-3}	2060	1.89×10^{-1}	2.10×10^{-3}	0.88	7.05×10^{-4}	1.02×10^{-5}
12	2410	1173	1.8×10^{-3}	4099	3.09×10^{-2}	1.64×10^{-1}	0.72	8.46×10^{-2}	1.70×10^{-5}
22	2830	1376	1.5×10^{-3}	4665	3.64×10^{-4}	1.91×10^{-1}	0.62	1.86×10^{-1}	1.50×10^{-5}
31	3110	1472	1.4×10^{-3}	4932	1.35×10^{-4}	1.91×10^{-1}	0.53	2.82×10^{-1}	1.33×10^{-5}
37	3778	2049	1.1×10^{-3}	5113	2.02×10^{-4}	1.91×10^{-1}	0.49	3.15×10^{-1}	7.49×10^{-6}

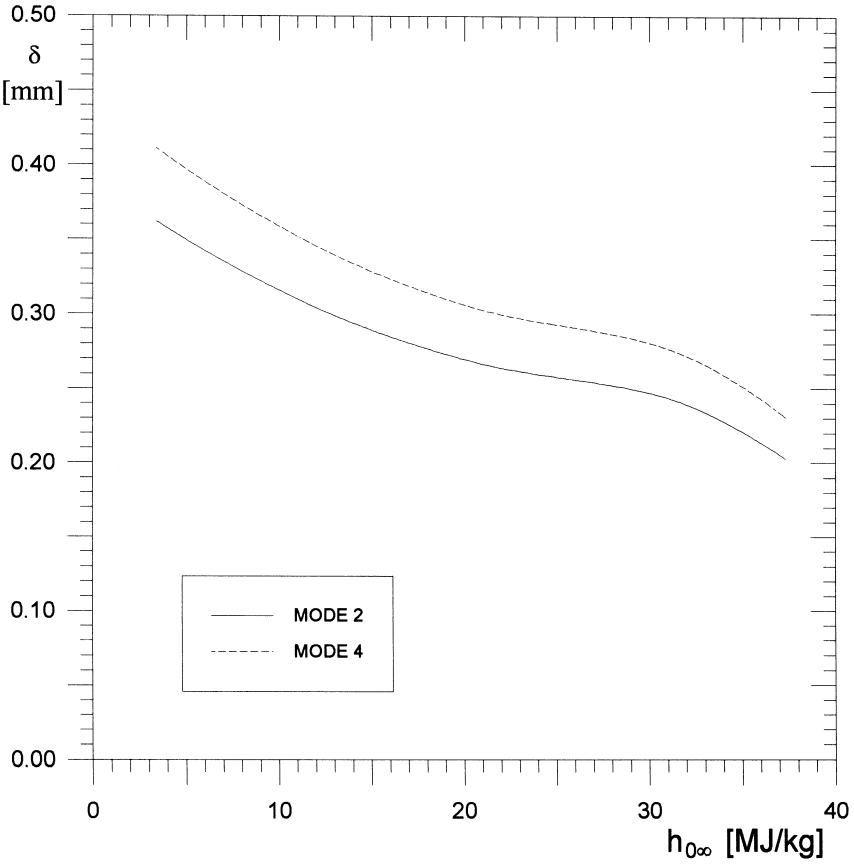

Fig. 2. Thickness of boundary layer at the stagnation point of a spherical body vs free stream total enthalpy.

$$\dot{q}_N = \dot{q}_w \sqrt{\frac{R_b}{p_s}} \tag{31}$$

where $\dot{q}_w$ is in W/cm^2, R_b is in cm and p_s is in atm. Use of $\dot{q}_N$ is useful to compare heat flux measurements, obtained in different test conditions.

The numerical results (almost ninety) were computed by De Filippis [11] and De Filippis et al. [12] by a Navier–Stokes code (H2NS), run in the range of enthalpy potential from 2 to 34 MJ/kg, considering a non-equilibrium boundary layer and a fully catalytic wall. H2NS is a hypersonic CFD code simulating both internal and external flows. The code has been developed at CIRCA (Centro Italiano Ricerche Aerospaziali) to foresee the performance of SCIROCCO (a high enthalpy arc wind tunnel in building phase at CIRA) and to evaluate the pressure and the heat flux peaks on spherical models. H2NS solves the full Navier–Stokes equations both in two-dimensional and axial-symmetric flow. The gas is a mixture of O_2, N_2, O, N and NO in chemical and vibrational non-equilibrium. This code has been widely validated both by reliable Navier–Stokes codes (e.g. VIRGINI [13]) and by experimental data [14].

The experimental heat fluxes are both from wind tunnels and ballistic ranges. All tests were made in air. The heat flux was measured by a calorimetric gage, mounted at the stagnation point of hemisphere cylinders. The wind tunnel data are by Rose and Stark [15] and by Horton and Babineaux [16]. Both sets of measurements were made in arc-driven shock tubes. Rose and Stark [15] carried out a specific analysis to determine the thermo-chemical state of air. The analysis relied on the comparison of measured heat fluxes with the results by the Fay–Riddell correlation formulas. The conclusion was that air was in equilibrium. Horton and Babineaux [16] did not perform such an analysis. The ballistic range data are by Yee et al. [17]. The measurements were made at an ambient temperature of 300 K and ambient pressure of 0.1 atm. According to the Yee et al. opinion [17], for these conditions the stagnation density is so high (approximately atmospheric) that the flow in the shock layer is in equilibrium. The equilibrium state of the test gas can be

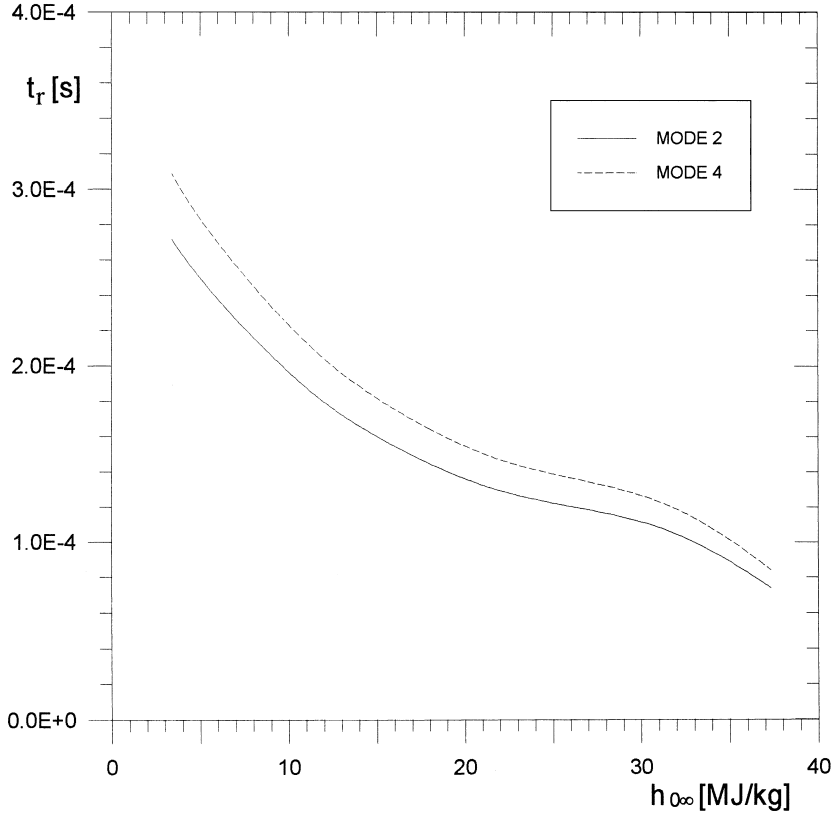

Fig. 3. Reference time vs free stream total enthalpy.

considered reasonably close to the state of the gas at a fully catalytic wall; these experimental heat fluxes can be used to compare the present numerical results.

7. Analysis of results

Figs. 2 and 3 show the profiles of boundary layer thickness at the stagnation point of a spherical body and of reference time, both as a function of the free stream total enthalpy, respectively. Computations have been made with: $x = 5 \times 10^{-5}$ m, $\eta_\delta = 3$, $df/d\eta = 1$ (i.e. non-dimensional velocity at the boundary layer edge). The value of x can be considered small enough, in fact, as the radius of the nose of a simulated body is 4.4×10^{-2} m then $x \cong 10^{-3} R_b$. The code was run in four operating modes:

Table 2
Wall boundary conditions

	Mode 1			Mode 4		
$h_{0\infty}$ [MJ/kg]	$d^2f/d\eta^2$	$d\vartheta/d\eta$	$dC_A/d\eta$	$d^2f/d\eta^2$	$d\vartheta/d\eta$	$dC_A/d\eta$
3	4.93×10^{-1}	3.14×10^{-1}	9.70×10^{-4}	4.93×10^{-1}	3.12×10^{-1}	8.30×10^{-4}
12	4.13×10^{-1}	3.04×10^{-1}	7.98×10^{-2}	4.18×10^{-1}	3.00×10^{-1}	6.80×10^{-2}
22	3.74×10^{-1}	2.96×10^{-1}	1.15×10^{-1}	3.73×10^{-1}	2.75×10^{-1}	9.80×10^{-2}
31	3.52×10^{-1}	2.93×10^{-1}	1.40×10^{-1}	3.51×10^{-1}	2.68×10^{-1}	1.20×10^{-1}
37	3.23×10^{-1}	2.78×10^{-1}	1.39×10^{-1}	3.22×10^{-1}	2.54×10^{-1}	1.20×10^{-1}

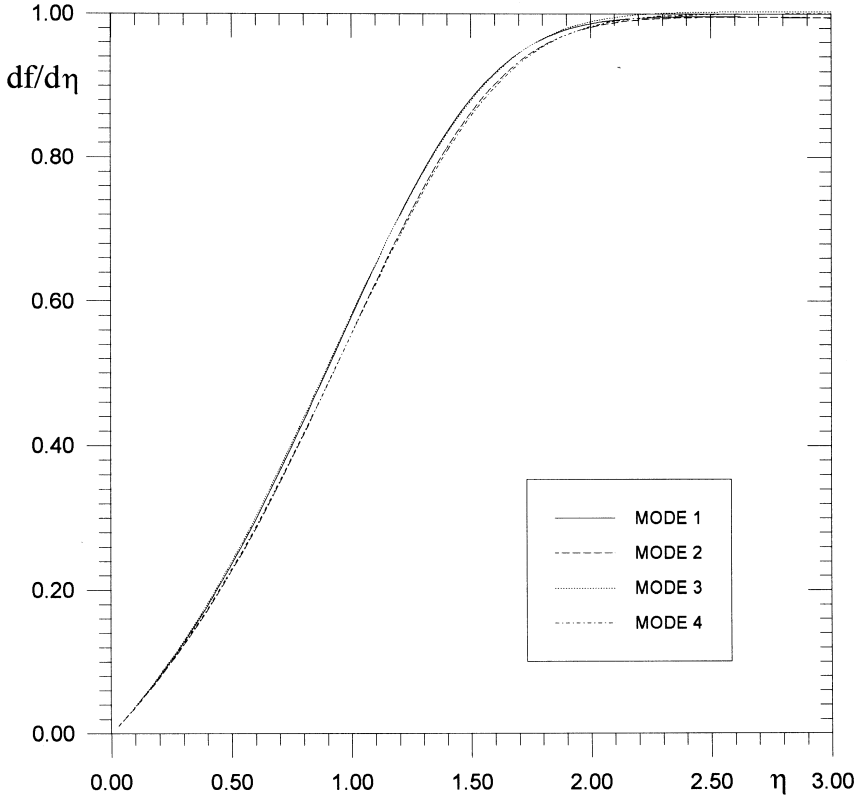

Fig. 4. Non-dimensional velocity profiles in the boundary layer: $h_{0\infty}=31$ MJ/kg.

- Mode 1: vibrational temperature constant in the boundary layer and Lennard–Jones collision integrals;
- Mode 2: vibrational temperature variable in the boundary layer and Lennard–Jones collision integrals;
- Mode 3: vibrational temperature constant in the boundary layer and Yun–Mason collision integrals;
- Mode 4: vibrational temperature variable in the boundary layer and Yun–Mason collision integrals.

Eqs. (2)–(4) have been integrated by a fourth-order Runge–Kutta algorithm. The numerical integration suffers from the shortcoming that the wall boundary conditions: $d^2f/d\eta^2$, $d\vartheta/d\eta$, $dC_A/d\eta$ are unknown. It has been necessary to use the numerical iterative procedure 'shooting technique' [2,4] to fix the values of the unknown boundary conditions, starting from guessed values. The convergence criterion of the shooting technique was 10^{-3}. Table 2 shows the values of the wall boundary conditions for the extreme operating conditions, i.e. Modes 1 and 4.

Figs. 4–7 show, for each operating mode and for $h_{0\infty}=31$ MJ/kg, the profiles of non-dimensional velocity ($df/d\eta$), non-dimensional temperature (ϑ), atom mass fraction (C_A) and mass fraction (C) of each chemical species as a function of η. As the mass fraction of nitrogen oxide is negligible, it is not reported in Fig. 7. The profiles of these parameters, that can be considered as examples of the boundary layer solution, look to be not strongly affected either by the variability of the vibrational temperature and by the transport model.

A stronger incidence of both these factors has to be pointed out on the distribution of the Lewis and Prandtl numbers. The profiles of these numbers, as a function of η and for $h_{0\infty}=31$ MJ/kg, are reported in Figs. 8 and 9, respectively. According to the hypothesis of a fully catalytic wall (the gas composition at the wall is the same) and of constant wall temperature, both Prandtl and Lewis numbers at the wall, are, respectively, the same for each operating mode. The Prandtl number is about 0.74, the Lewis number is about 1.0. For Modes 1 and 2 these numbers show a monotone trend and reduction of 6 and 36%, respectively, from the wall to the boundary layer edge. For Modes 3 and 4, both the Prandtl and Lewis numbers show a relative maximum, located at $\eta\cong 0.73$ and 0.56, respectively. Free stream Prandtl and Lewis numbers

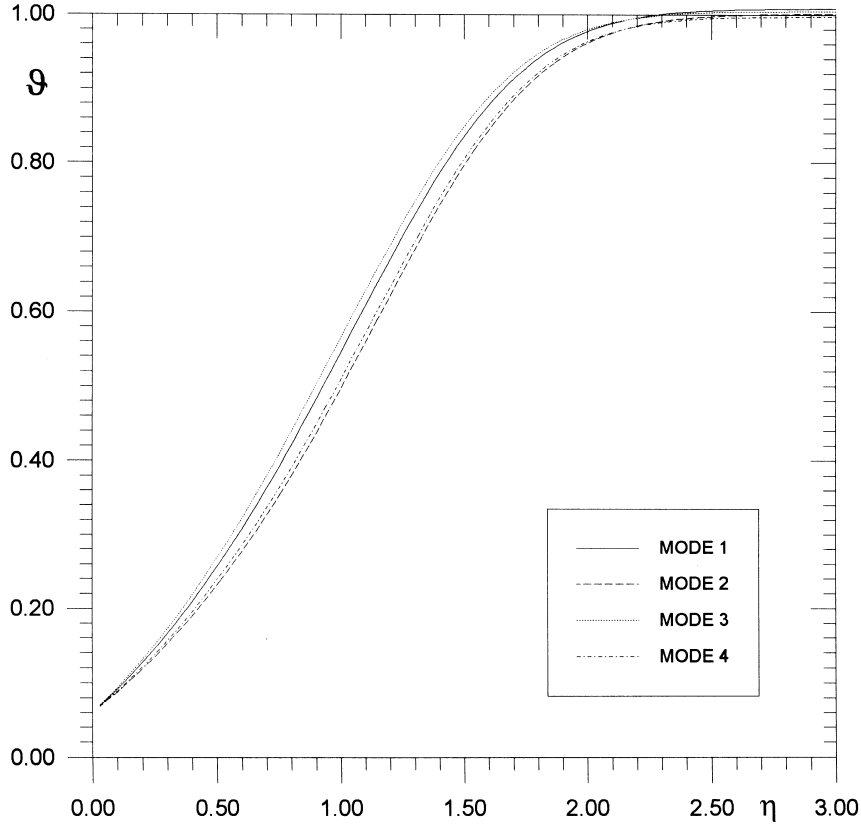

Fig. 5. Non-dimensional temperature profiles in the boundary layer: $h_{0\infty} = 31$ MJ/kg.

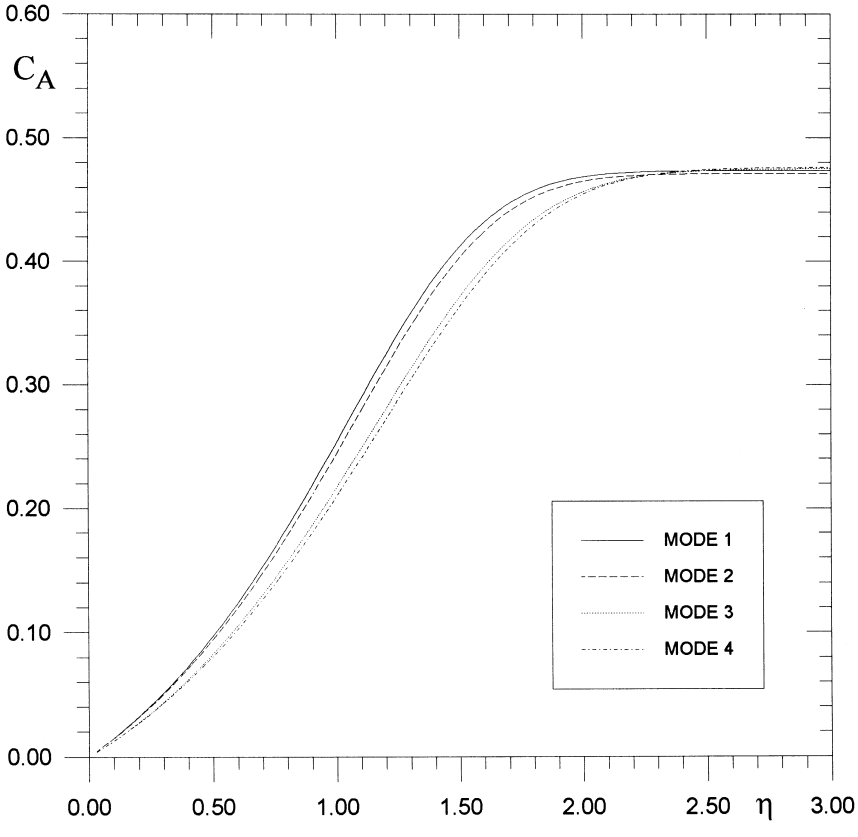

Fig. 6. Atom mass fraction profiles in the boundary layer: $h_{0\infty} = 31$ MJ/kg.

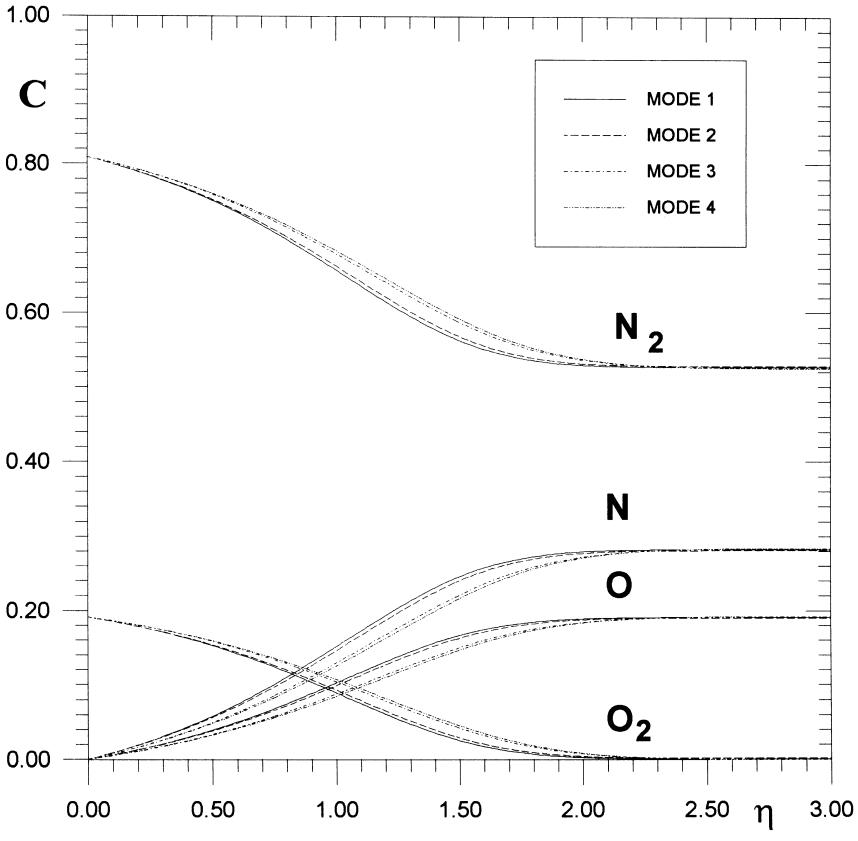

Fig. 7. Mass fraction profiles in the boundary layer: $h_{0\infty} = 31$ MJ/kg.

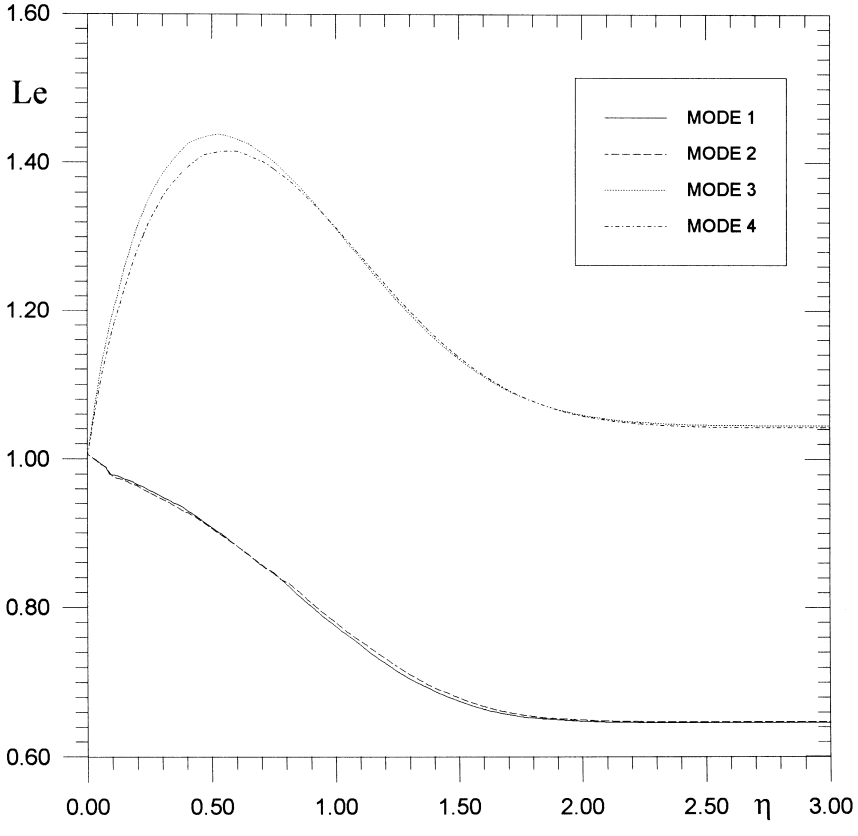

Fig. 8. Lewis number profiles in the boundary layer: $h_{0\infty} = 31$ MJ/kg.

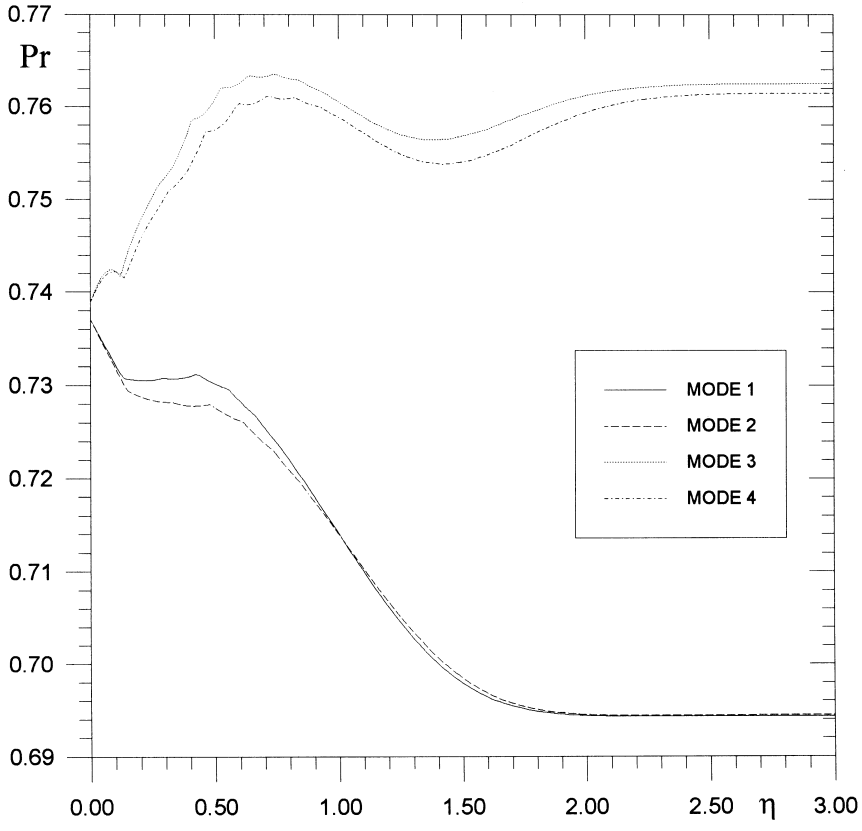

Fig. 9. Prandtl number profiles in the boundary layer: $h_{0\infty} = 31$ MJ/kg.

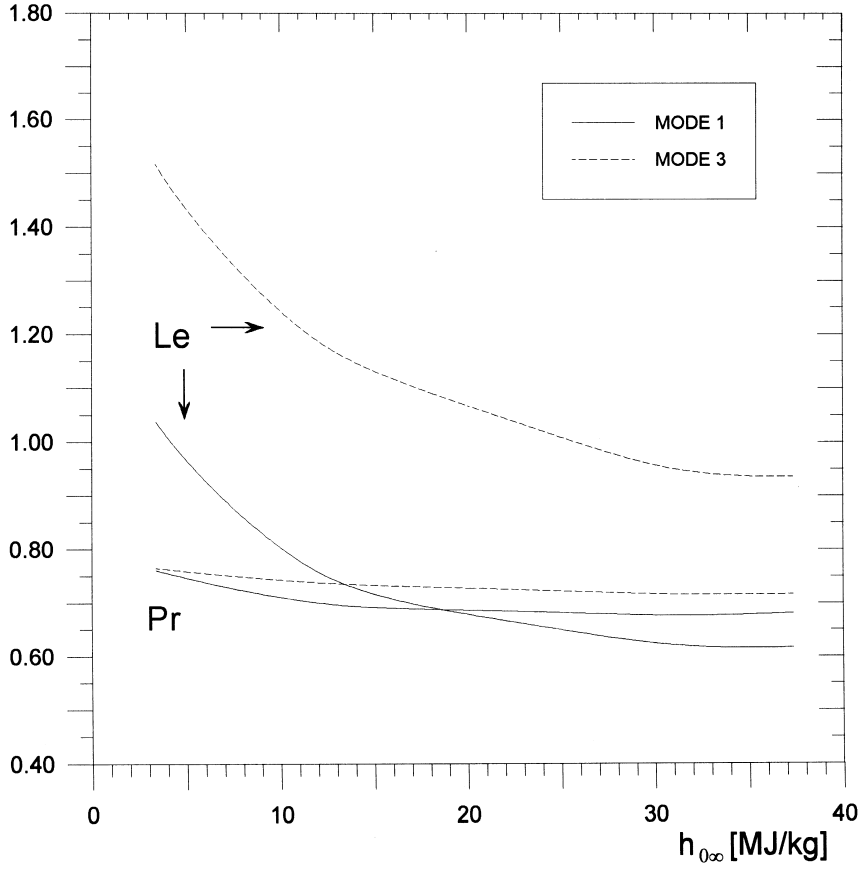

Fig. 10. Free stream Prandtl and Lewis numbers vs free stream total enthalpy.

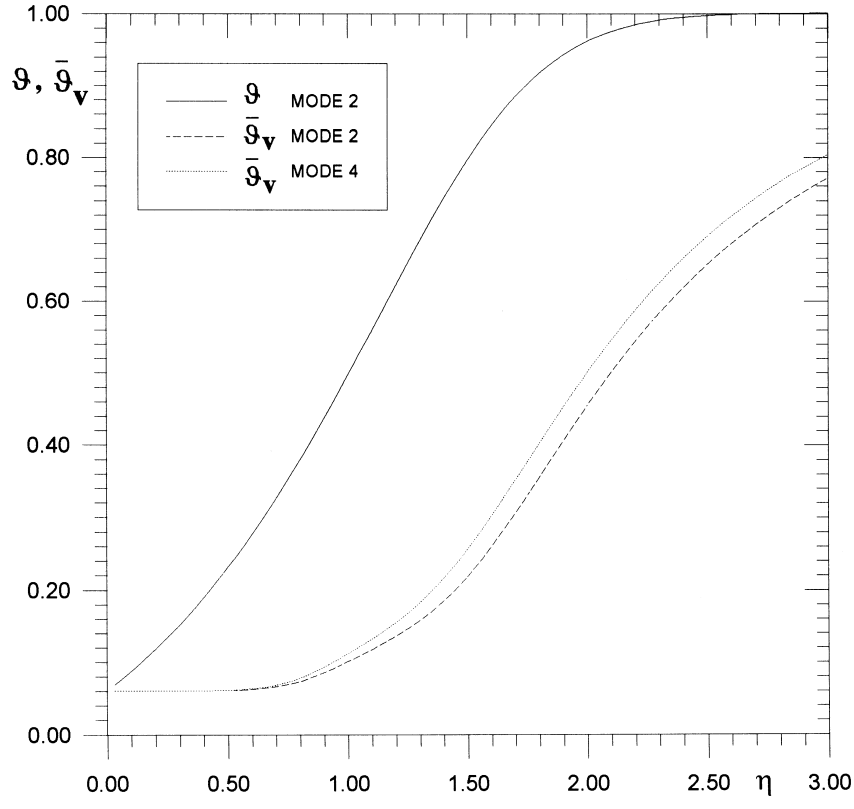

Fig. 11. Non-dimensional temperature profiles: $h_{0\infty} = 31$ MJ/kg.

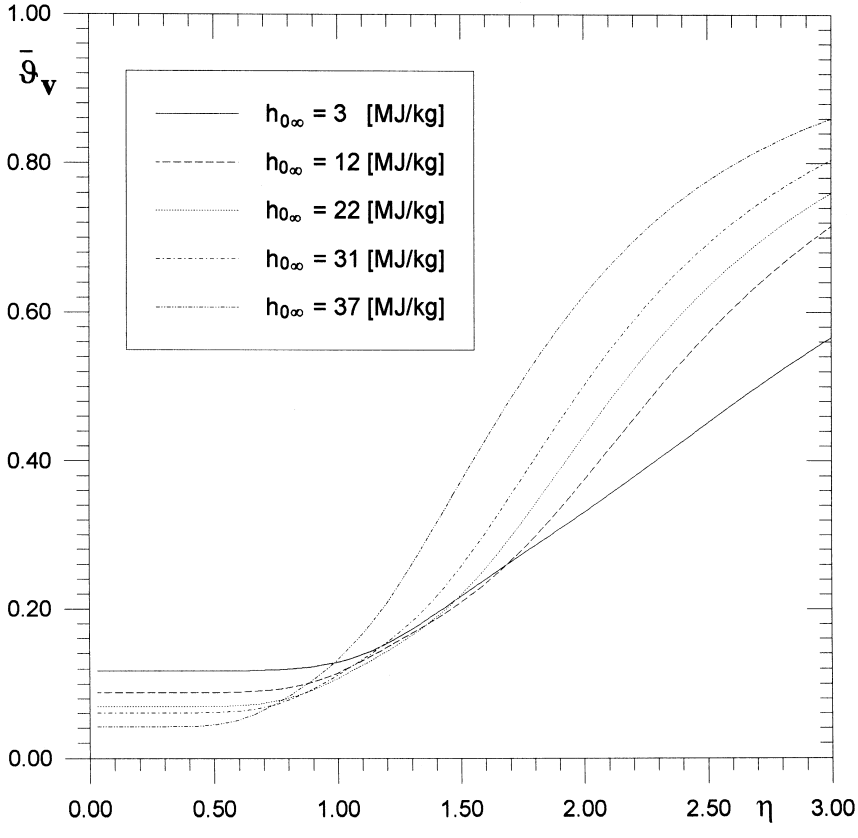

Fig. 12. Non-dimensional vibrational temperature profiles by Mode 4.

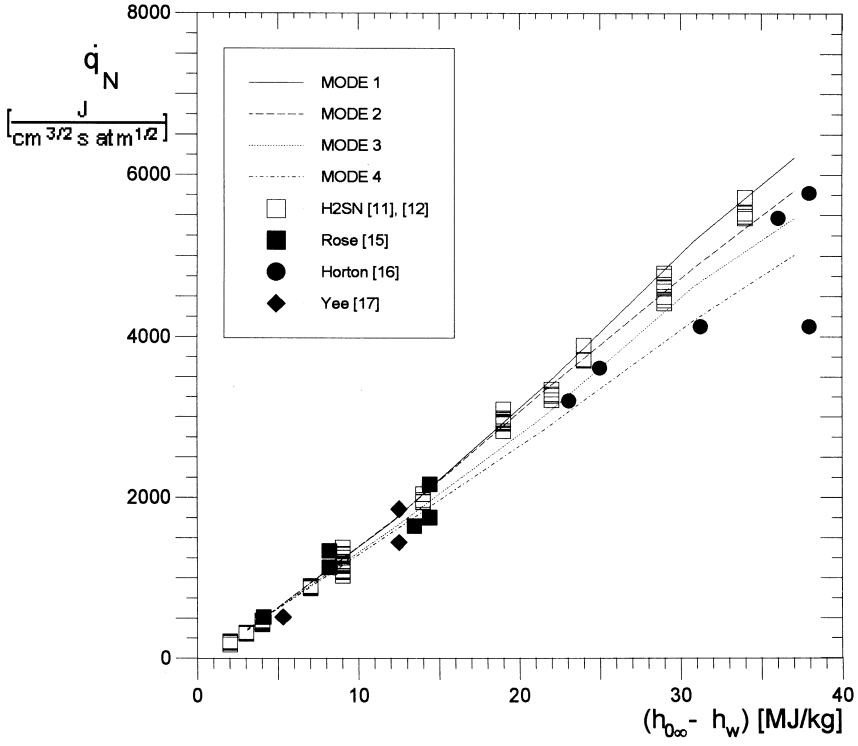

Fig. 13. Normalized heat fluxes vs enthalpy potential.

are reported in Fig. 10 for Modes 1 and 3, as a function of the free stream total enthalpy. For both operating modes the Prandtl and Lewis numbers reduce roughly by the same amount. In fact the Prandtl number reduces by 11 and 6%, and the Lewis number by 41 and 38% for Modes 1 and 3, respectively.

The profiles of average, non-dimensional, vibrational temperature in the boundary layer and, by comparison, of non-dimensional thermodynamic temperature, for $h_{0\infty} = 31$ MJ/kg, are reported in Fig. 11. The transport model does not strongly influence the values of the vibrational temperature. The mismatch between ϑ and $\bar{\vartheta}_v$ indicates that the molecular vibration process does not reach an equilibrium state. The profiles of non-dimensional, vibrational temperature in the boundary layer by Mode 4, for each enthalpy level are shown in Fig. 12. As expected both the vibrational temperature and the slope of the profile increase with the free stream total enthalpy.

The comparison of normalized heat fluxes is shown in Fig. 13. Considering as reference results those obtained by Mode 1, one can point out that up to an enthalpy potential of about 22 MJ/kg, the variability of vibrational temperature does not strongly influence the heat flux (Mode 2). As expected, at higher values of total enthalpy, the molecular vibration process is more endothermic, giving rise to a reduction of the heat flux. This reduction ranges, for enthalpy potential from 22–37 MJ/kg, between 2 and 7%. The influence of the collision integrals is similar to one of the variation of vibrational temperature (Mode 3). In fact the heat flux reduces, in the whole enthalpy range, from 0–12%. The synergetic effect of the two factors (Mode 4) produces a reduction of the heat flux, in the whole range of enthalpy potential, from 0–19%.

A good compromise in the agreement with both H2SN results and experimental data is achieved by Mode 2 results. This indicates that the inclusion in the computing procedure, of the variability of the molecule vibration temperatures improves the simulation of the thermo-chemistry process. At the same time the Lennard–Jones collision integrals seem to suit the boundary layer solution better than the Yun–Mason collision integrals.

8. Conclusions

The incidence of the variability of molecule vibration in the boundary layer and of the transport model has been evaluated on the computation of both the boundary layer parameters and the wall heat flux. This evaluation has been performed by an improved version of the Fay–Riddell procedure, solving the laminar, steady

boundary layer at the stagnation point of spherical bodies, and computing the wall heat flux. Runs have been performed up to a free stream total enthalpy of about 40 MJ/kg. A non-equilibrium boundary layer and a fully catalytic wall have been considered.

As expected the inclusion in the computing procedure of the variability of the molecule vibration temperature improves the simulation of the thermochemistry process and therefore, the computation of the heat flux. The Lennard–Jones collision integrals seem to be more suitable than the Yun–Mason collision integrals for boundary layer solution.

The present procedure needs to be tested further by also considering other states of the gas (e.g. frozen and equilibrium boundary layer) and other wall boundary conditions (partially catalytic and non-catalytic wall).

References

[1] R.L. King A computer version of the US standard atmosphere, NASA CR-150778 1978.

[2] J.A. Fay, F.R. Riddell, Theory of stagnation point heat transfer in dissociated air, Journal of Aeronautical Sciences 25 (2) (1958) 73–85.

[3] G. Zuppardi, G. Verde, Improved Fay–Riddell procedure to compute the stagnation point heat flux, Journal of Spacecraft and Rockets 35 (3) (1998) 403–405.

[4] J.D. Anderson, in: Hypersonic and High Temperature Gas Dynamics, McGraw-Hill, New York, 1989, pp. 626–636.

[5] R.B. Bird, W.E. Stewartson, E.N. Lightfoot, in: Transport Phenomena, Ambrosiana, Milan, 1960, pp. 518–523 (in Italian).

[6] K.S. Yun, E.A. Mason, Collision integrals for the transport properties of dissociating air at high temperature, The Physics of Fluid 5 (4) (1962) 380–386.

[7] G. Zuppardi, G. Verde, An approximate method to evaluate the surface catalycity in high enthalpy flows, in: Proceedings of the 8th International Conference on Computation Methods and Experimental Measurements (CMEM '97), 1997 May.

[8] G. Zuppardi, G. Verde, A. Esposito Numerical modelling of an arc jet wind tunnel, Dipartimento di Scienza ed Ingegneria dello Spazio "Luigi G. Napolitano" Report J-96-1, Naples, 1996 (in Italian).

[9] D.L. Baulch, D.D. Drysdale, D.G. Home, A.C. Lloyds, in: Evaluated Kinetic Data for High Temperature Reactions, vol. 2, Butterworths, London, 1973.

[10] E.V. Zoby Empirical stagnation point heat transfer relation several gas mixtures at high enthalpy levels, NASA TN D-4799 1968.

[11] F. De Filippis, M. Serpico Air high enthalpy stagnation point heat flux calculation, Centro Italiano Ricerche Aerospaziali TN 96-014, Capua, 1996.

[12] F. De Filippis, A. Schettino, M. Serpico, S. Borrelli, Complete analytical model to describe the test-leg of Scirocco PWT, in: Proceedings of the 20th Congress of the International Council of the Aeronautical Sciences (ICAS-96) Sorrento, 1996.

[13] F. De Filippis, M. Serpico, M. Marini, M. Ravachol, J.P. Tribot, Comparison between numerical and experimental results on different HERMES elevon shapes, in: Proceedings of the 14th AIAA Applied Aerodynamics Conference, New Orleans, 1996.

[14] M. Serpico, A. Schettino, S. Borrelli Proceedings of MSTP Workshop 1996 on Re-entry Aero-thermodynamics and Ground-to-Flight Extrapolation. Contribution to Electre Model in F4 and HEG conditions, ONERA Technical Report RT 88/6121 SY, 1996.

[15] P.H. Rose, W.I. Stark, Stagnation point heat transfer measurements in dissociated air, Journal of Aeronautical Sciences 25 (2) (1958) 86–97.

[16] T.E. Horton, T.L. Babineaux, Influence of atmospheric composition on hypersonic stagnation-point convective heating, AIAA J. 5 (1) (1967) 36–43.

[17] L. Yee, H.E. Bailey, H.T. Woodward Ballistic range measurements of stagnation-point heat transfer in air and in carbon dioxide at velocities up to 18,000 feet per second, NASA TN D-777, 1961.